Remote Sensing Applications: Society and Environment 4 (2016) 109–118

Contents lists available at ScienceDirect

Remote Sensing Applications: Society and Environment

journal homepage: www.elsevier.com/locate/rsase

Improved water extraction using Landsat TM/ETM+ images in Ebinur Lake, Xinjiang, China

Fei Zhang [a,b,*], Tashpolat Tiyip [a,b], Hsiang-te Kung [c], Verner Carl Johnson [d], Juan Wang [a,b], Ilyas Nurmemet [a,b]

[a] Resources and Environment Department, Xinjiang University/Key Laboratory of Oasis Ecology, Ministry of Education, Urumqi 830046, PR China
[b] Key Laboratory of Oasis Ecology, Ministry of Education, Xinjiang University, Urumqi 830046, PR China
[c] Department of Earth Sciences, The University of Memphis, Memphis, TN 38152, USA
[d] Department of Physical and Environmental Sciences, Colorado Mesa University Grand Junction, CO 81501, USA

ARTICLE INFO

Article history:
Received 25 December 2015
Received in revised form
7 August 2016
Accepted 9 August 2016
Available online 10 August 2016

Keywords:
Water information
Spectral relationship
Ebinur Lake

ABSTRACT

Water is the most common and important resources on earth. In this paper, we tested and analyzed a variety of water indices for water surface extraction using Landsat TM/ETM+ images, and evaluated extraction accuracies over Ebinur Lake area in Xinjiang Uyghur Autonomous Region of China. Eleven algorithms found in literature on land surface water extraction, including normalized difference water index (NDWI), modified normalized difference water index (MNDWI), automatic water extraction index with no shadow ($AWEI_{nsh}$), automatic water extraction with shadow ($AWEI_{sh}$), vegetation index 1 (VI-1), vegetation index 2 (VI-2), vegetation index 3 (VI-3), water index (LBV_B), national wetland inventory (NWI), enhanced water index (EWI), and revised normalized different water index (RNDWI) were used. The results were validated by a maximum likelihood classification method, edge extraction accuracy assessment and extracted the area of Ebinur Lake from higher-resolution Landsat ETM+ panchromatic band. The results showed that these algorithms have different accuracies in extracting water information. We proposed VI-2 for $KT_3+TM_4 > TM_2+TM_7$ and VI-3 for $KT_3+TM_2 > TM_4+TM_3$ as an optimized and comprehensive method for land surface water extraction from Landsat TM/ETM+ Images (KT_3, i.e. Wetness index from the Kauth-Thomas Transformation). The proposed VI-2 and VI-3 models demonstrated its potential in water body extraction with 92.95% and 85.04% accuracies, outperforming other algorithms. Using the optimal mask water model, the two models achieved up to 93.80% accuracy while minimizing the disturbance from vegetation and non-exploited land. Through comparison with other commonly used methods, it shows that the performance of the proposed method is superior to the others. Therefore VI-2 and VI-3 are the best indicators for water mapping using Landsat TM/ETM+ images. This study provided its great potential for quantitative evaluating of temporal changes of Ebinur Lake in Xinjiang Uyghur Autonomous Region of China.

1. Introduction

Water is one of the most important natural resources for human survival (Ridd and Liu, 1998). Surface waters such as lakes, rivers, artificial reservoirs, and seas are essential for climate equilibrium, hydrological cycle as well as ecosystem balance, providing fundamental resources to terrestrial life (Tulbure and Broich, 2013; Verpoorter, et al., 2014). Information accuracy about the spatial distribution of land surface water is imperative for assessment of water resources, watershed changes, land surface water management as well as environmental monitoring (NRC, 2008; Sun et al., 2012).

In recent decades, remote sensing (RS) technology has become an essential tool in monitoring water information (Senthilnath et al., 2012; Kodikara et al., 2011; Muster et al., 2013; El-Asmar and Hereher, 2011; Rokni et al., 2014). Lakes in arid climatic regions with a valley/basin are the last link between natural water circulation and human economic activity systems. Water statistics are supportive in understanding the ecological and environmental changes of the inland river basins (Bhasang et al., 2012). These systems are likely to be the first reaction to disturbances from humans. The development of remote sensing technology, monitoring techniques of lake waters have advanced from the traditional hydrometrical station to more comprehensive monitoring, combined with stream-flow measuring and remote sensing

* Corresponding author at: Resources and Environment Department, Xinjiang University/Key Laboratory of Oasis Ecology, Ministry of Education, Urumqi 830046, PR China.
E-mail address: zhangfei3s@163.com (F. Zhang).

http://dx.doi.org/10.1016/j.rsase.2016.08.001
2352-9385/

imaging (McFeeters, 1996; Feyisa et al., 2014; Alanazi and Ghrefat, 2013; Huang et al., 2012; Ma et al., 2014). Landsat images have frequently been used to extract water bodies. The methods can be summarized into three classes: single wavelength threshold, multi-wavelength spectral relationship, and the water index method (Rundquist et al., 1987; Alesheikh et al., 2007; Zhang, 2008). The single wavelength threshold method is simple in operation, but creates noise which makes the identification resolution low. The multi-wavelength spectral relationship and the water index methods are widely used to obtain water information. A number of researchers have utilized various methods to study water body extraction methods. For example, McFeeters (1996) utilized the normalized different water index (NDWI) to restrain the vegetation and ground samples to extract water information. In the research of the Wagga Lake region of Australia, Frazier and Page, 2000 pointed out TM_5 threshold segmentation with a higher accuracy in water extracted samples, but failed to include small water samples. Yang et al. (2010) applied ETM+ defined thresholds and automated extraction methods for small water bodies in the mountainous areas of south China. Guo et al. (2012) took the relationship of various water index models and investigated other methods to define the thresholds for water extraction of image binarization methods. Hassani et al. (2015) developed an index of water surfaces (IWS) for separating the water surfaces from other types of land use by using the images of Landsat 7 ETM+.

As a result of the dry riverbeds, sedimentation in the water, aquatic vegetation, and shallow water depth will generate diverse spectral patterns. These produce certain disturbances for the extracted water samples. Fig. 1 summarizes the reflectance characteristics of the samples. *"The clear water reflectance is lower than that of the vegetation, urban, mountain shadow, and mixed water categories. Because of the reflectance pattern for mountain shadows was similar to the pattern for the water, which may lead to confusion between these categories during automated image processing"* (Feyisa et al., 2014). However, it is worth noting that the clear water reflectance is higher than that of the mountain shadow in Band 1 through Band 3 and opposite is true for the longer bands. In addition, the spectral absorption intensity ratio of the water body is larger than others on the near infrared (NIR) and shortwave Infrared (SWIR) wavelengths of Landsat TM/ETM+ images. Even if the water is very shallow, reflection energy is low, and other features, such as vegetation and bare soil, in these two band energy absorption is lesser, reflection energy is higher, which makes the water body on NIR and SWIR wavelengths have the obvious difference with other features. So the NIR and SWIR wavelength can be used to eliminate the interference of water bodies by threshold segmentation method. The turbid water reflectance increased with the presence of hydrophytes and sediments on the lake (Jiang et al., 2014).

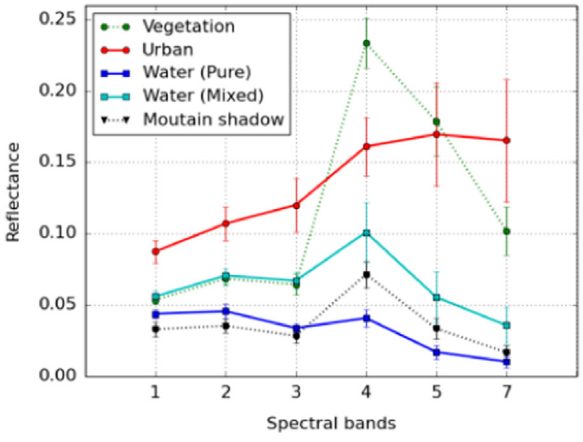

Fig. 1. Means and standard deviations of surface reflectance in the five lands cover types (Jiang et al., 2014).

Asphalt pavements and shadows cause errors in the identification of water bodies, which is common when used optical remote sensing images. To effectively extract the water samples of enclosed lakes, we used Landsat TM/ETM+ images from the United States Geological Survey (USGS, 2012) over Ebinur Lake and surrounding areas, the largest salt-water lake in Xinjiang Uyghur Autonomous Region of China. Eleven water extraction indices including single wavelength threshold method, and multi-band spectral methods, and new index was proposed in this study that demonstrated an improved accuracy over the existing methods.

2. Study area

Ebinur Lake is located between 44°43′N and 45°12′N latitude and 82°35′E and 83°11′E longitude. The lake is situated next to Gurbantunggut Desert in the east, close to Tuoli County in the north, and adjacent to Republic of Kazakhstan in the northwest. Ebinur Lake Wetland National Nature Reserve has a high concentration of many types of desert plants and also serves as an important habitat for birds in the northwestern part of Xinjiang (Qian et al., 2004) (Fig. 2). In this area, the average temperature is 7.36 °C; the mean annual precipitation is 149 mm; and annual potential evaporation is 2281 mm. It belongs to a typical temperate continental climate (Yuan and Zhang, 2010). Within one year, about 72 days have the highest temperatures being between 30–35 °C, 15 days with 35–40 °C, and about 2 days with greater than 40 °C. Also about 88 days have lowest temperatures between −20 to −10 °C, 39 days with −30 to −20 °C, and about 2 days with less than −30 °C. Three major rivers, Boertala, Jinghe, and Kuitun, flow into Ebinur Lake. In the past several decades, the lake area has reduced and the exposed lakebed has grown larger. As a result is the area around Ebinur Lake is a major source of dust, which impacts the ecological environment of northern Xinjiang Province.

3. Data and methods

3.1. Data

Landsat ETM+ images collected on September 5, 2011, and Landsat TM collected on September 6 and 13, 2011 at path/row of 145/29 and 146/29, respectively were used for this study. The TM/ETM+ images were acquired from USGS GLOVIS (http://glovis.usgs.gov/). All Landsat images used are corrected and cloud free. TM/ETM+ images acquired in the form of digital number (DN) were calibrated to surface reflectance values (Wang et al., 2006). Atmospheric correction was applied to all images using the Fast Line-of-Sight Atmospheric Analysis of Spectral Hypercube (FLAASH) tool in ENVI 5.1 (Feyisa et al., 2014; Estoque and Murayama, 2015). The images were mosaicked to generate new images covering the entire study area. For this reason, a mosaicking tool based on geo-referenced images was used. For co-registration of the multi-temporal images, one of the images was used as the reference to register the other images. The input images were co-registered with a root mean square error (RMSE) of less than 0.5 pixels. Finally, the Nearest Neighbor method was used to resample the data (Rokni et al., 2015). In this study, each image pixel is 30 m × 30 m, and study area has 7391 × 2137 pixels.

3.2. Land surface water extraction

Numerous methods have been developed to delineate water information in remote sense imagery (Table 1). The most

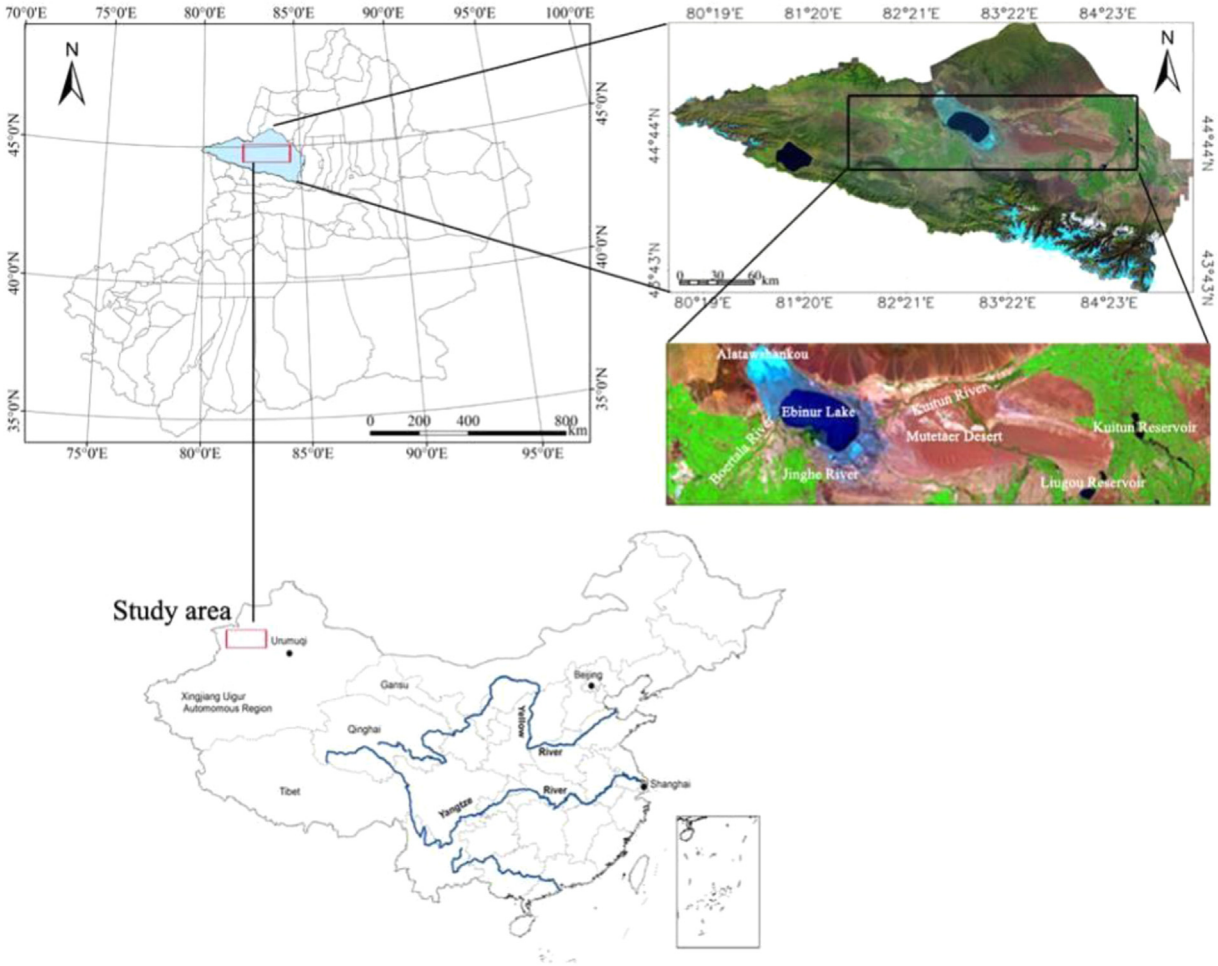

Fig. 2. Location of the study area.

commonly used methods include: (1) Spectral bands which identify water information by applying thresholds to one or more spectral bands which is easy to implement, but often misclassify mountain shadows, urban areas and water body (Rundquist et al., 1987); (2) Classification methods based on supervised or unsupervised machine-learning algorithms to extract water bodies from multi-spectral imagery (Otukei and Blaschke, 2010); and (3) Water indices (WIs) derived from two or more spectral bands that enhance the difference between water body and land use/cover types (Townshend and Justice, 1986). However, the WIs are widely used because of their relatively high accuracy in water information detection. For this paper the summary of the Landsat TM images of the Ebinur Lake for extracting water body sample methods in remotely sensed imagery are specified in Table 1.

3.3. Accuracy verification for classification

A quantitative assessment of the accuracy was conducted for the study area. The overall accuracy and the kappa coefficient on the basis of the error matrix (Foody, 2002) were employed to evaluate the accuracy of maximum likelihood classification map. The kappa coefficient can be calculated as:

Table 1
Summary of land surface water information acquiring methods.

Number	Water information acquiring methods	Formulation
1	NDWI	(TM_2-TM_4) / (TM_2+TM_4) (McFeeters, 1996; Brakenridge and Anderson et al., 2006)
2	MNDWI	(TM_2-TM_5) / (TM_2+TM_5) (Tebbs et al.,2013)
3	$AWEI_{nsh}$	$4\times(\rho_{TM2}-\rho_{TM5})-(0.25\rho_{TM4}+2.75\times\rho_{TM7})$ (Feyisa et al., 2014)
4	$AWEI_{sh}$	$\rho_{TM1}+2.5\times\rho_{TM2}-1.5\times(\rho_{TM4}+\rho_{TM5})-0.25\rho_{TM7}$ (Feyisa et al., 2014)
5	Vegetation index 1 (VI-1)	(TM_1-TM_7) /(TM_1+TM_7) (Wu et al.,2013)
6	Vegetation index 2 (VI-2)	$KT_3+TM_4>TM_2+TM_7$ (Liu, et al., 2013)
7	Vegetation index 3 (VI-3)	$KT_3+TM_2>TM_4+TM_3$ (Liu, et al., 2013)
8	LBV_B	$1.126971\times TM_2+0.673348\times TM_3+0.077966\times TM_4-1.878287\times TM_5+159$ (Liu et al., 2013)
9	NWI	$(TM_1-(TM_4+TM_5+TM_7))$ / $(TM_1+(TM_4+TM_5+TM_7))\times C$ (Liu, et al., 2013) (C is constant, in this study, the C=10)
10	EWI	$(TM_2-TM_4-TM_5)$ / $(TM_2+TM_4+TM_5)$ (Yan et al., 2007)
11	RNDWI	(TM_5-TM_3) / (TM_5+TM_3) (Wu et al., 2013)

Note: NDWI: Normalized Difference Water Index; MNDWI: Modified Normalized Difference Water Index; $AWEI_{nsh}$: Automated Water Extraction Index with no shadow; $AWEI_{sh}$: Automated Water Extraction Index with shadow; LBV_B: radiance Level, Balance and Variation vector_Balance; NWI: New Water Index; EWI: Enhanced Water Index; RNDWI: Revised Normalized Difference Water Index, the same as follows.

$$Kappa = \frac{P\sum_{i=1}^{n} P_{ii} - \sum_{i=1}^{n}(P_{i+} \times P_{+i})}{P^2 - \sum_{i=1}^{n}(P_{i+} \times P_{+i})} \quad (1)$$

where P is the total number of pixels from the reference data; P_{ii} is the total number of correct pixels from the category; P_{i+} is the total number of pixels for the category derived from the classified data; P_{+i} is the total number of pixels for the category derived from the reference data; and n is the total number of categories.

3.4. Water area extraction

Visual interpretation and quantitatively statistical analysis methods are used to analyze and precisely evaluate the areas of water body from various models. According to Ma et al. (2014) research, the water area can be calculated as:

$$S = S_w + S_m \quad (2)$$

where S is the total water area, S_w is the area of pure water; and S_m is the water area in the mixed pixels. In this study, according to the condition of the study area, the area calculation of water body is based on Eq. (3) from Jiang et al. (2013)

$$S = \sum_{i=1}^{N} pixelSize \times pixelSize \times 10^{-6} \quad (3)$$

where *S* is the total water area of Ebinur Lake; *N* is the pixel numbers; and *pixelSize* is the resolution of images. Water extraction results of various models were overlaid with the original images, through visual inspection and on the basis of Maximum Likelihood Classification. Joint validation was conducted for water extraction accuracy of the proposed method.

3.5. Accuracy of the edge for the extracted Ebinur Lake

Boundary extraction is a simple morphological image processing algorithm that extracts the outermost pixels of features from a binary image (Gonzalez et al., 2009). Two metrics were applied to evaluate the results from different perspectives:

$$E_C = N_C/N_R \times 100\% \quad (4)$$

$$E_O = N_O/N_R \times 100\% \quad (5)$$

here, E represents the edge position error frequency (C for commission and O for omission), N_R is the number of edge pixels in the reference image; N_C is the number of extracted edge pixels that lie outside the reference water bodies (i.e., the number of commission errors); and N_O is the number of extracted edge pixels that lie inside the reference water bodies and that are not directly adjacent to the actual edge (i.e., omission errors). In this study, each image pixel is 30 m × 30 m, so the Eqs. (4) and (5) are valid for 30 m pixel. Fig. 3 shows methods adopted in this study to extract land surface water information.

4. Results

4.1. Land surface water extraction

Using the Landsat TM data of Ebinur Lake, eleven common algorithms shown in Table 1 were used for extracting water body. Results are shown in Fig. 4. We found VI-2 and VI-3 methods performed well in extracting water from the Landsat TM data and partially eliminating the impact of mountain shadows.

Furthermore, the detailed comparison of water bodies,

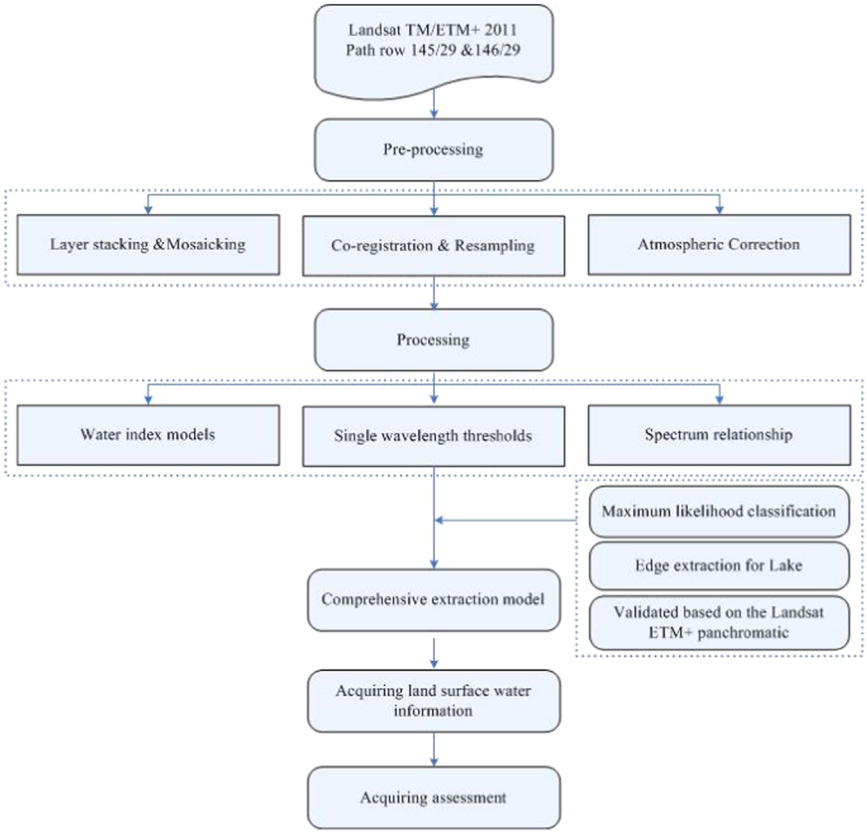

Fig. 3. Flowchart showing the overall methods adopted in this study.

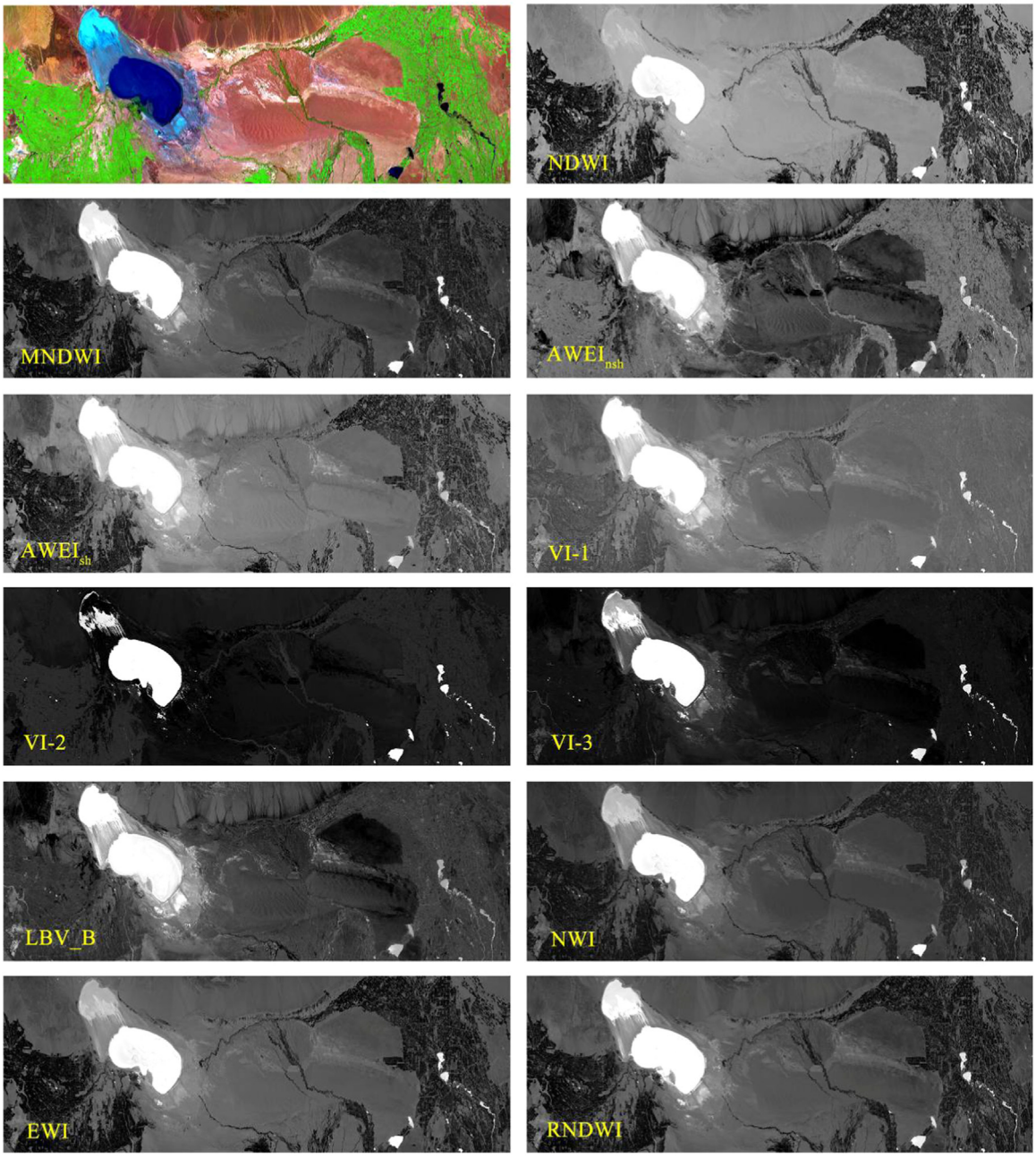

Fig. 4. Comparison of different land surface water information map of various extraction methods in the study area.

vegetation cover, and non-exploited ground from these eleven algorithms is listed in the Fig. 5. In the red elliptical area, VI-2 and VI-3 water extraction models suppressed vegetation information more effectively, which increased the accuracy of the water body extraction by lowering the mixing of water and non-water covered ground. Furthermore the images of other models have lower identification of water, vegetation cover, and non-exploited ground. The water information could not be extracted exactly and therefore the accuracy of water information acquiring was lower.

4.2. Maximum likelihood classification

Maximum likelihood classifier is one of the most commonly used methods in land use/cover classification. (Feyisa et al., 2014; Frazier and Page, 2000). It was easy to find visual differences between water and shadows in stretched water image derived using threshold technique in SWIR band, in which some shadow pixels were present. Therefore, the method of maximum likelihood classification could be used to classify the water image (Du et al., 2002). We classified the remote sensing images into two parts: water body and others (farmland, forestland, grassland, etc.) (Fig. 6). According to the Eq. (1), we obtained classification overall accuracy of 99.3% and the kappa coefficient of 0.99. Also from calculation using Eq. (3) water body area was estimated at 55.35×10^7 km^2. These results indicated the classification was very accurate.

The threshold method is considered a common approach to extract water bodies because it is easier to use and less computationally time-consuming than alternatives approaches (Ryu et al., 2002). In this study, to determine the optimal threshold, a series of thresholds were tested and each possible threshold generates a water body extraction result. Because a higher threshold may identify only a few water bodies, a lower threshold may not only identify many water bodies, but also mistakenly

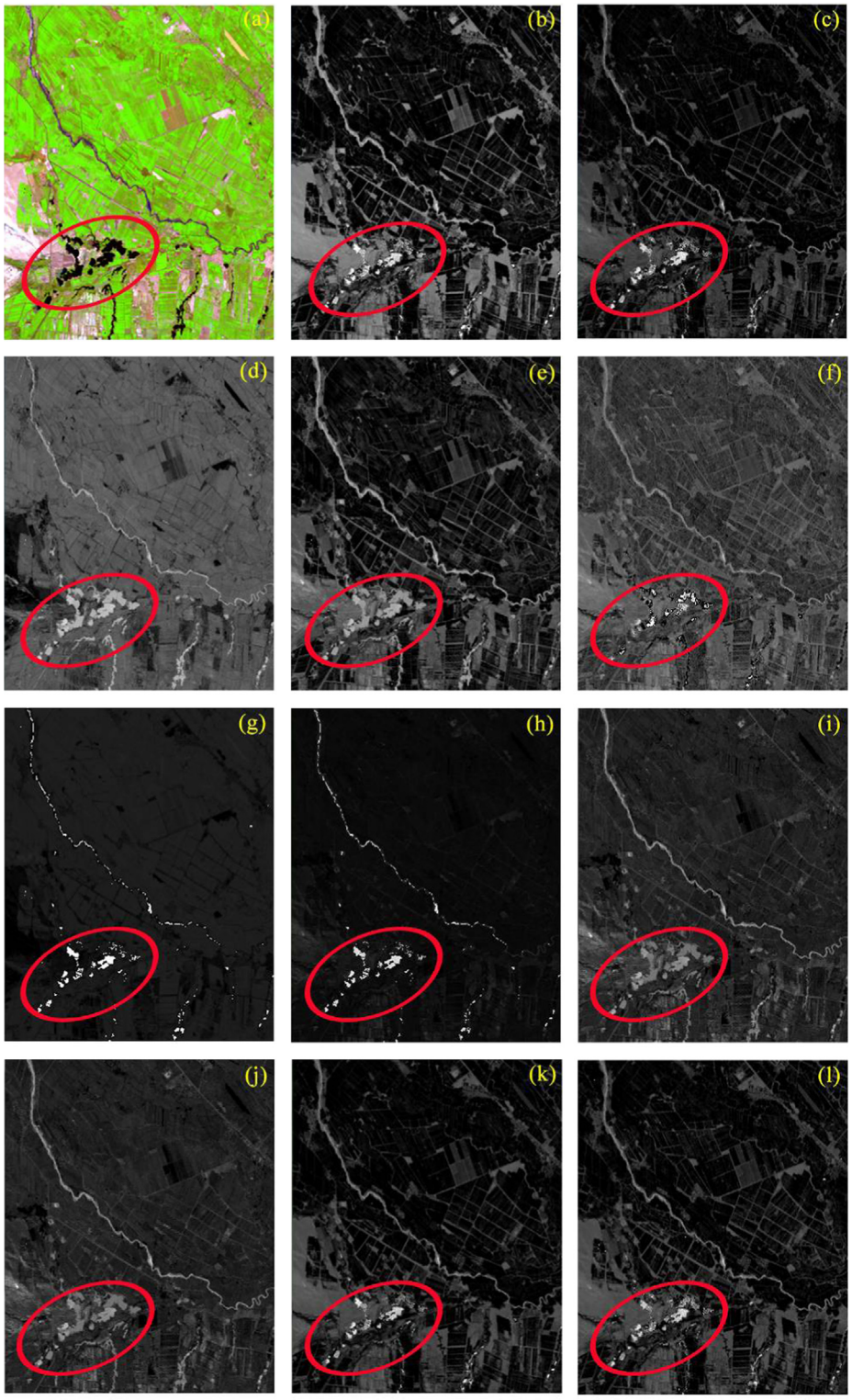

Fig. 5. Comparison between Landsat TM image and land surface water information map of various extraction models. a: Original image, b: NDWI, c: MNDWI, d: $AWEI_{nsh}$, e: $AWEI_{sh}$, f: Vegetation index 1 (VI-1),g: Vegetation index 2 (VI-2), h: Vegetation index 3 (VI-3), i: LBV_B, j: NWI, k:EWI, l:RNDWI. (For interpretation of the references to color in this figure, the reader is referred to the web version of this article.)

identify land as water bodies. So, according to the tested thresholds for all water indices, we obtained the optimal thresholds for each index, and the extraction results of eleven indices were presented in Table 2.

The results indicate the accuracy of water area from various water body extraction models. The accuracy for VI-2 was the highest at 92.95%. The second highest accuracy was VI-3 at 85.04%. These results for VI-2 and VI-3 were in consistent with in-situ measurements and validation index highlighting the potential to provide more accurate water information from Landsat data.

Nevertheless, the method of threshold for discriminating water body from other land covers is somewhat dependent on human experience, thus influencing the accuracy of image classifications. To further evaluate the accuracy of water indices, Landsat ETM+

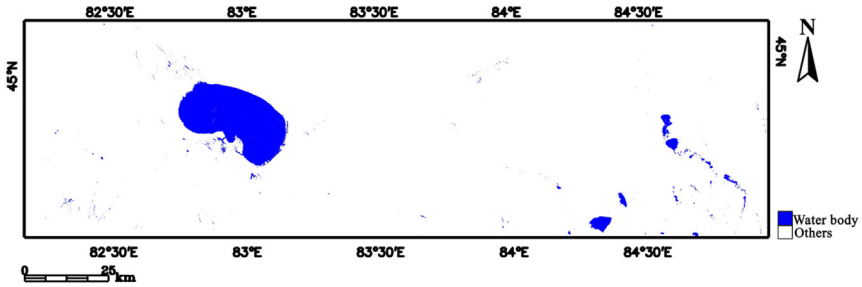

Fig. 6. Maximum likelihood classification map.

Table 2
The results and accuracy evaluations of water information extraction models.

Number	Land surface water information extraction methods	Optimal threshold	Models area (m^2)	Classification area (m^2)	Accuracy (%)
1	NDWI	0.00	65.55×10^7	55.35×10^7	84.44
2	MNDWI	0.32	81.83×10^7		67.64
3	$AWEI_{nsh}$	0.00	87.10×10^7		63.55
4	$AWEI_{sh}$	0.20	75.65×10^7		73.17
5	Vegetation index 1 (VI-1)	0.30	86.30×10^7		64.14
6	Vegetation index 2 (VI-2)	0.20	59.55×10^7		92.95
7	Vegetation index 3 (VI-3)	1.03	65.09×10^7		85.04
8	LBV_B	159.08	99.84×10^7		55.44
9	NWI	−5.00	94.91×10^7		58.32
10	EWI	−0.10	72.26×10^7		76.60
11	RNDWI	−0.20	89.54×10^7		61.82

panchromatic was used to identify the edges of the Ebinur Lake manually and the lake edge image was used as reference image. We choose 200 points at the edges of Ebinur Lake to identify the mixed pixels.

Table 3 summarizes the edge extraction accuracy for Ebinur Lake. It can be seen that there still either high commission or omission errors at the edges in some water index results regardless of a suitable threshold. According to the results, the VI-2 and VI-3 showed smaller error of lake boundary extraction. The reason for this result is that the VI-2 and VI-3 are more vulnerable to shadow pixels than the others.

The area of Ebinur Lake was validated using the Landsat ETM+ panchromatic band which offers a higher spatial resolution. The lake shoreline was delineated manually on-screen from the reference data. Furthermore, the result was used to assess the accuracy of the indices of water body (Table 4). The accuracy for VI-2 was the highest at 95.12%. The second highest accuracy was with the VI-3 at 94.46%. That result is the same as the maximum likelihood classification validation results that the accuracy of the VI-2 and VI-3 methods are considerably higher than the others. So, the maximum likelihood classification method is feasible in this study area. The image used in this analysis was clipped from the image for study area and shown in Fig. 7.

Table 3
Edge extraction accuracy assessment for Ebinur Lake. E: errors (C, commission; O, omission).

Number	Land surface water information extraction methods	Ec (%)	Eo (%)
1	NDWI	3.0	35.0
2	MNDWI	5.0	50.5
3	$AWEI_{nsh}$	5.5	57.0
4	$AWEI_{sh}$	9.5	36.0
5	Vegetation index 1 (VI-1)	2.5	56.5
6	Vegetation index 2 (VI-2)	4.0	22.5
7	Vegetation index 3 (VI-3)	4.5	26.5
8	LBV_B	2.5	60.0
9	NWI	5.0	58.5
10	EWI	11.5	34.0
11	RNDWI	5.0	61.5

4.3. Comprehensive extraction method of land surface water information

There were no clear boundaries between vegetation cover, river-beds and water bodies in the study area. All three of these features generated errors of thresholds which are difficult to differentiate the mixed pixels exactly. In order to solve some of the problems of the traditional water extraction, model can hardly extract small and tiny water body, according to discrepancy between water body and non-water body. We selected VI-2 and VI-3 to complement the distinctions between water body and non-water-body, for example water from the vegetation cover (see flowchart in Fig. 8). Based on both of these methods, according to the scope of the research region, the accuracy of comprehensive method was obtained by the estimated water areas divided by the water areas from the maximum likelihood classification.

Wu et al. (2008) proposed a multiplication method to optimize water extraction model. Two image masks were multiplied (i.e. $B1 \times B2$), if the water was presented in both masks, the value would be one; otherwise it would be zero. This procedure reduced the spatial information and increased the water extraction accuracy. In this proposal, the space information is reduced, which improves the accuracy of land surface water information (Fig. 9). Using an optimized mask, through Eq. (3), the calculated water body area is 59.01×10^7 m^2 and compared to the classification result, the accuracy is 93.80%. It is concluded that the comprehensive water extracted model provided better information on water and reduced the confusion of water and other ground object in the Landsat TM data. Thus accuracy was greatly improved after adopting the comprehensive extracted method.

5. Discussion

Many researchers used water extracted methods based mainly on a single model using only spectral data and it is not suitable for

Table 4
Precision of extraction of the area of Ebinur Lake.

Number	Land surface water information extraction methods	Optimal threshold	Models area (m^2)	Reference area from ETM+ Panchromatic (m^2)	Accuracy (%)
1	NDWI	0.00	4.82×10^8	4.51×10^8	93.13
2	MNDWI	0.32	5.21×10^8		84.48
3	$AWEI_{nsh}$	0.00	5.34×10^8		81.60
4	$AWEI_{sh}$	0.20	4.79×10^8		93.79
5	Vegetation index 1 (VI-1)	0.30	5.27×10^8		83.15
6	Vegetation index 2 (VI-2)	0.20	4.73×10^8		95.12
7	Vegetation index 3 (VI-3)	1.03	4.76×10^8		94.46
8	LBV_B	159.08	5.43×10^8		79.60
9	NWI	−5.0	5.29×10^8		82.70
10	EWI	−0.10	4.78×10^8		94.01
11	RNDWI	−0.20	5.67×10^8		74.28

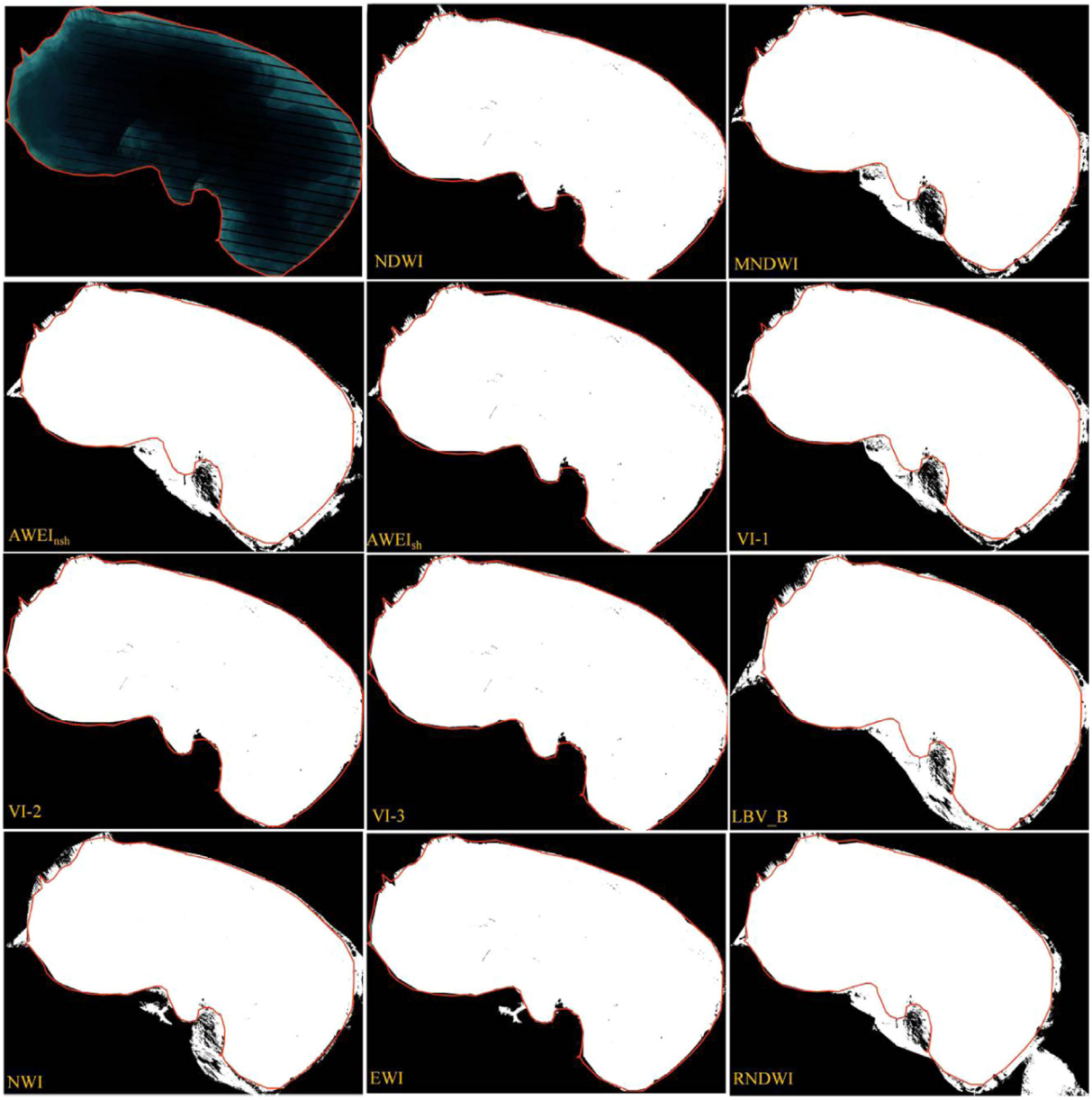

Fig. 7. Comparison of the area of Ebinur Lake between Landsat ETM+ image and various extraction models.

complicated areas such as Ebinur Lake. These methods do have inherent deficiencies. For example, using differ extraction methods specified in Table 2, the results showed the overall accuracy of water information extraction varied between 55.44% and 92.95%. These ranges of accuracy indicated that there were some misclassifications in the land surface and water maps. This misclassification may have been caused by overestimation of small water bodies and underestimation of the river channels with

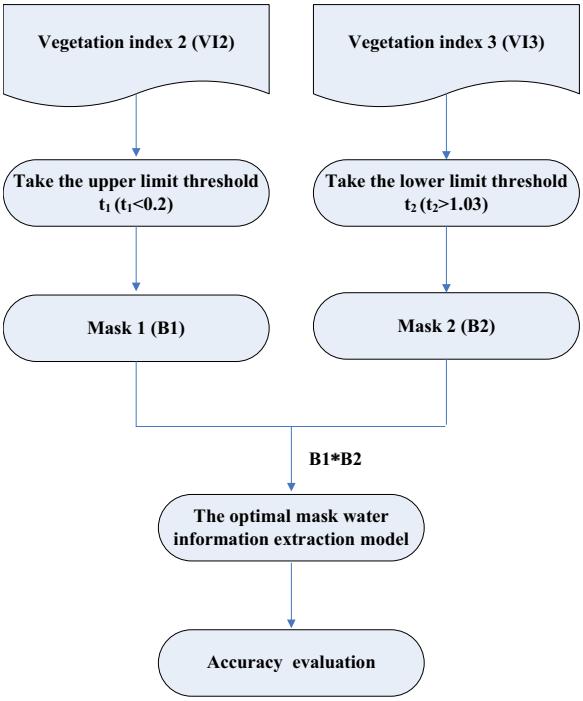

Fig. 8. Technique flow chart of the comprehensive method.

mixed pixels. This can be addressed by using spectral linear unmixing methods by Keshava and Mustard (2002).

One factor that may significantly affect the efficiency of land surface water maps is the threshold selection which is influenced by the subjective judgment of the researcher. Another major factor is the absence of ground-truth water body surface distribution and area data. To solve this problem, high-resolution data should be used. Additionally, the Landsat-8 Operational Land Imager (OLI) may provide an important data source for a better estimation of water bodies due to its multiple spectral bands within water sensitive wavelengths as specified below:

(1) Due to the water extraction indices were developed on specific areas of interests, there were significant differences exist among the results of various water extraction indices. Therefore, the selection of proper models or the assembling of water models is extremely important (Song et al., 2014; Rokni et al., 2015)
(2) The salinized land, such as dry riverbeds with silt and aquatic plants/hydrophytes has certain disturbances for water body spectrum. This disturbance generates the deviation of water information estimation. So, the application of multi-temporal remote sensing information and the study of water identification models should provide guidance to solve the problems.
(3) Estimation accuracy of small-water bodies is a current bottleneck in remote sensing of water resources. According to Liu (2013), there are certain spectral similarities between shadows and water features. The accuracy of water identification is mainly influenced by shadow noise. Therefore, efforts should be made to reduce or eliminate shadow noise from the water extraction indices.

6. Conclusion

In this study, we conducted a comparative study among eleven water indices by using visual interpretation and quantitative statistical analysis. Our results showed that all eleven models can automatically extract water information to some degree. The results were validated by using maximum likelihood classification, edge extraction accuracy assessment and Ebinur Lake water body area derived from 15 m Landsat ETM+ pan band. VI-2 and VI-3 models proposed in this study, demonstrated the highest accuracy in the identification of water body. So VI-2 and VI-3 models are more suitable for the water information extraction of Ebinur Lake. These two models utilize the visible and near infrared wavebands. It provides references for the water information automatic extraction from the images of National China-Brazil Earth Resources Satellite and Environment & Disaster Monitoring Small Satellite.

In the eco-tone areas, the complexity of no clear boundaries of vegetation cover, river-beds, and water bodies often causes larger errors due to mixed pixel effect. It is difficult to exactly differentiate objects in mixed pixels. To improve the extraction accuracy of small water bodies using the common water body models, we proposed VI-2 and VI-3 as an optimized method of extracting water information. The calculated water area is 59.01×10^7 m^2 and the accuracy is 93.80% to compare with classification result. This method utilizes the comprehensive water extraction model and provides much better water information.

Overall, the VI-2 and VI-3 algorithms can extract surface water information more accurately than the other methods. Also these methods are suitable for the surface water extraction from Landsat TM images. The results of other models are not very good because some small water bodies could not be effectively extracted from Landsat TM images. Thus further study is needed in other areas for water information extraction, because the proposed approach has proven to be effective in detecting the land surface water information of Ebinur Lake in our study. Accordingly, the research project method may also be useful in studying other land surface water questions (such as flood monitoring) in the world.

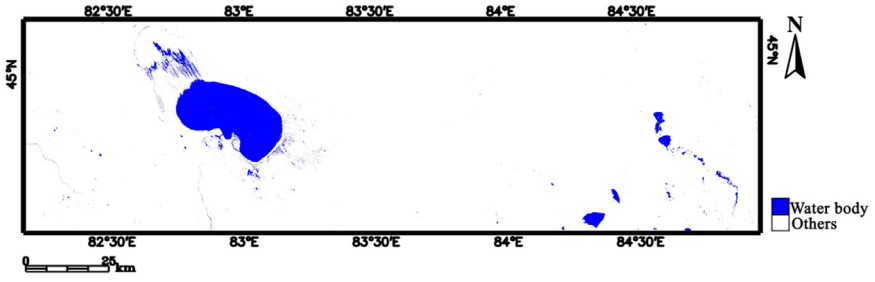

Fig. 9. Water information extraction result of the comprehensive method.

Acknowledgments

We are grateful to the financial support provided by the National Natural Science Foundation of China (No. 41361045), Xinjiang Local Outstanding Young Talent Cultivation Project of National Natural Science Foundation of China (U1503302), the Young Technology-Innovation Training Program Foundation for Talents from the Xinjiang Uygur Autonomous Region (No. 2013731002), the National International Scientific and Technological Cooperation Projects (No. 2010DFA92720-12), the State Key Program of National Natural Science of China (No. 41130531), the Key Laboratory of Oasis Ecology in Xinjiang University (No. XJDX0201-2012-01). We wish to thank Professor Bethany Iris LaGrone, Julia Shena Crutchfield, Spencer Colton, and other referees for providing helpful suggestions to improve this manuscript.

References

Alanazi, H.A., Ghrefat, H.A., 2013. Spectral analysis of multispectral Landsat 7 ETM+ and ASTER data for mapping land cover at Qurayah Sabkha, Northern Saudi Arabia. J. Indian Soc. Remote Sens. 41 (4), 833–844.

Alesheikh, A.A., Ghorbanali, A., Nouri, N., 2007. Coastline change detection using remote sensing. Int. J. Environ. Sci. Technol. 4, 61–66.

Bhasang, T., Liu, J.S., Niu, J.F., Dhawa, T., Bian, C., 2012. Area variation and its causes of Bamu Co Lake in the Central Tibet. J. Nat. Resour. 27 (2), 302–310 (in Chinese).

Brakenridge R., Anderson E., 2006. MODIS-based flood detection, mapping and measurement: The potential for operational hydrological applications. In: Transboundary Floods: Reducing Risks Through Flood Management, pp. 1–12.

Du, J.K., Feng, X.Z., Wang, Z.L., Huang, Y.S., Ramadan, E., 2002. The methods of extracting water information from SPOT image. Chin. Geogr. Sci. 12 (1), 68–72.

El-Asmar, H.M., Hereher, M.E., 2011. Change detection of the coastal zone east of the Nile Delta using remote sensing. Environ. Earth Sci. 62, 769–777.

Estoque, R.C., Murayama, Y.J., 2015. Classification and change detection of built-up lands from Landsat-7 ETM+ and Landsat-8 OLI/TIRS imageries: a comparative assessment of various spectral indices. Ecol. Indic. 56, 205–217.

Feyisa, G.L., Meilby, H., Fensholt, R., Proud, S.R., 2014. Automated water extraction index: a new technique for surface water mapping using Landsat imagery. Remote Sens. Environ. 140, 23–35.

Foody, G.M., 2002. Status of land cover classification accuracy assessment. Remote Sens. Environ. 80, 185–201.

Frazier, P.S., Page, K.J., 2000. Water body detection and delineation with Landsat TM data. Photogramm. Eng. Remote Sens. 66 (12), 1461–1467.

Gonzalez, R.C., Woods, R.E., Eddins, S.L., 2009. Digital Image Processing Using MATLAB. Gatesmark Publishing Knoxville, Knoxville, TN, USA, p. 2009.

Guo, Z.Y., Wang, X.Y., Wang, C.H., Gao, C., Wu, H.Z., 2012. The research on extraction method of water body information in Chaohu Lake Basin. Remote Sens. Technol. Appl. 27 (3), 443–448 (in Chinese).

Hassani, M., Chabou, M.C., Hamoudi, M., Guettouche, M.S., 2015. Index of extraction of water surfaces from Landsat 7 ETM+ images. Arab. J. Geosci. 8 (6), 3381–3389.

Huang, J.L., Tao, H., Wang, Y.J., Bai, Y.G., 2012. Analysis on relationship between water level and water area of lake based on MODIS image. Trans. Chin. Soc. Agric. Eng. 28 (23), 140–146 (in Chinese).

Jiang, H., Fen, M., Zhu, Y.Q., Lu, N., Huang, J.X., Xiao, T., 2014. An automated method for extracting rivers and lakes from Landsat Imagery. Remote Sens. 6 (6), 5067–5089.

Jiang, L.G., Yao, Z.J., Liu, z F., Wu, S.S., 2013. A review of lake dynamic change research based on remote sensing. Remote Sens. Technol. Appl. 28 (5), 807–814 (in Chinese).

Keshava, N., Mustard, J.F., 2002. Spectral unmixing. IEEE Signal Process. Mag. 19, 44–57.

Kodikara, R.L., Woldai, T., Ruitenbeek, F.J.A., Kuria, Z., Meer, F., Shepherd, K.D., Hummel, G.J., 2011. Hyperspectral remote sensing of evaporate minerals and associated sediments in Lake Magadi Area, Kenya. Int. J. Appl. Earth Obs. Geoinf. 14 (1), 22–32.

Liu, G.L., Zhang, L.C., Liu, J., Li, G.Y., 2013. Water body information extraction based on Landsat TM remote sensing imagery. J. Univ. Chin. Acad. Sci. 30 (5), 644–650 (in Chinese).

Ma, B.D., Wu, L.X., Zhang, X.X., Li, X.C., Liu, Y., Wang, S.L., 2014. Locally adaptive unmixing method for lake-water area Extraction based on MODIS 250m bands. Int. J. Appl. Earth Obs. Geoinf. 33, 109–118.

McFeeters, S.K., 1996. The use of the Normalized Difference Water Index (NDWI) in the delineation of open water features. Int. J. Remote Sens. 17 (7), 1425–1432.

Muster, S., Heim, B., Abnizova, A., Boike, J., 2013. Water body distributions across scales: a remote sensing based comparison of three arctic tundra wetlands. Remote Sens. 5, 1498–1523.

National Research Council, 2008. Integrating Multiscale Observations of U.S. Waters. The National Academies Press, Washington, DC, USA.

Otukei, J., Blaschke, T., 2010. Land cover change assessment using decision trees, support vector machines and maximum likelihood classification algorithms. Int. J. Appl. Earth Obs. Geoinf. 12, 27–31.

Qian, Y.B., Wu, Z.N., Jiang, J., Yang, Q., 2004. Eco-environmental change and its impact factors in the Ebinur Lake catchments during the past 50 years. J. Glaciol. Geocryol. 26 (1), 17–26 (in Chinese).

Ridd, M.K., Liu, J., 1998. A comparison of four algorithms for change detection in an urban environment. Remote Sens. Environ. 63, 95–100.

Rokni, K., Ahmad, A., Selamat, A., Hazini, S., 2014. Water feature Extraction and change detection using multi-temporal Landsat imagery. Remote Sens. 6, 4173–4189.

Rokni, K., Ahmad, A., Solaimani, K., Hazini, S., 2015. A new approach for surface water change detection: Integration of pixel level image fusion and image classification techniques. Int. J. Appl. Earth Obs. Geoinf. 34, 226–234.

Rundquist, D.C., Lawson, M.P., Queen, L.P., Cerveny, R.S., 1987. The relationship between summer-season rainfall events and lake-surface area. J. Am. Water Resour. Assoc. 23, 493–508.

Ryu, J.H., Won, J.S., Min, K.D., 2002. Waterline extraction from Landsat TM data in a tidal flat: a case study in Gomso Bay, Korea. Remote Sens. Environ. 83, 442–456.

Senthilnath, J., Bajpai, S., Omkar, S.N., Diwakar, P.G., Mani, V., 2012. An approach to multi-temporal MODIS image analysis using image classification and segmentation. Adv. Space Res. 50, 1274–1287.

Song, C.Q., Huang, B., Ke, L.H., Richards, K.S., 2014. Remote sensing of alpine lake water environment changes on the Tibetan Plateau and surroundings: a review. ISPRS J. Photogramm. Remote Sens. 92, 26–37.

Sun, F., Sun, W., Chen, J., Gong, P., 2012. Comparison and improvement of methods for identifying waterbodies in remotely sensed imagery. Int. J. Remote Sens. 33, 6854–6875.

Tebbs, E.J., Remedios, J.J., Avery, S.T., Harper, D.M., 2013. Remote sensing the hydrological variability of Tanzania's Lake Natron, a vital lesser flamingo breeding site under threat. Ecohydrol. Hydrobiol. 13, 148–158.

Tulbure, M.G., Broich, M., 2013. Spatiotemporal dynamic of surface water bodies using Landsat time-series data from 1999 to 2011. ISPRS Journal of Photogrammetry and Remote Sensing 79, 44–52.

Townshend, J.R., Justice, C., 1986. Analysis of the dynamics of African vegetation using the normalized difference vegetation index. Int. J. Remote Sens. 7, 1435–1445.

United States Geological Survey (USGS), 2012. Landsat Data Archive. Global Visualization Viewer (GLOVIS).

Verpoorter, C., Kutser, T., Seekell, D.A., Tranvik, L.J., 2014. A global inventory of lakes based on high-resolution satellite imagery. Geophys. Res. Lett. 41, 6396–6402.

Wang, F., Han, L., Kung, H.T., Van Arsdale, R.N., 2006. Applications of Landsat-5 TM imagery in assessing and mapping water quality in Reelfoot Lake, Tennessee. Int. J. Remote Sens. 27 (23), 5269–5283.

Wu, J.T., Tan, W., Yu, L.F., 2013. Comparative study of different water indexes based on TM/ETM+ imagery. Sci. Surv. Mapp. 38 (4), 193–195 (in Chinese).

Wu, W.Y., Shen, X.H., Zhou, L.J., Lu, S.L., Zhang, G.F., 2008. A Integrated method for water body detection delineation using Landsat ETM+ data. Bull. Sci. Technol. 24 (2), 252–259 (in Chinese).

Yan, P., Zhang, Y.J., Zhang, Y., 2007. A study on information extraction of water system in semi-arid regions with the Enhanced Water Index (EWI) and GIS based noise remove techniques. Appl. Remote Sens. 6, 62–67 (in Chinese).

Yang, S.W., Xue, C.S., Liu, T., 2010. A method of small water information automatic extraction from TM remote sensing images. Acta Geod. Cartogr. Sin. 39 (6), 611–617 (in Chinese).

Yuan, X.C., Zhang, L.P., 2010. Analysis of hydrological characteristics of Xinjiang River Basin in Jinghe. Mod. Agric. Sci. Technol. 6 (1), 289–294 (in Chinese).

Zhang, M.H., 2008. Extracting water-body information with improved of spectral relationship in a higher mountain area. Geogr. Geo-Inf. Sci. 24 (2), 14–16 (in Chinese).